Mechanical Systems and Signal Processing 249 (2026) 114082

Contents lists available at ScienceDirect

Mechanical Systems and Signal Processing

journal homepage: www.elsevier.com/locate/ymssp

Full length article

# Fractional modeling of nonlinear ship rolling dynamics under evolutionary and irregular sea-wave loads

Ioannis P. Mitseas

*School of Civil Engineering, University of Leeds, Leeds, LS2 9JT, UK*

ARTICLE INFO

Communicated by I. Kougioumtzoglou

*Keywords:*
Ship rolling dynamics
Fractional calculus
Stochastic averaging
Statistical linearization
Stochastic process
Memory effects

ABSTRACT

This paper presents an efficient semi-analytical methodology for determining the non-stationary response of ships undergoing nonlinear rolling under stochastic sea-wave excitations. The dynamic response is captured through a comprehensive and physically consistent nonlinear formulation that incorporates both softening and hardening restoring moment characteristics, non-conventional fractional-order hydrodynamic damping mechanisms that naturally embed memory effects, and non-stationary stochastic wave loads representative of complex maritime environments. By leveraging a refined blend of stochastic averaging and statistical linearization the proposed stochastic fractional-order framework delivers computationally efficient, time-dependent second-order response statistics together with fully non-stationary roll angle amplitude probability-density surfaces. Tailored weighting factors and fractional derivative orders allow flexible tuning of restoring and damping characteristics to represent a wide range of relevant ship roll dynamics. Numerical analyses across a range of case studies, validated against benchmark Monte Carlo simulations, demonstrate the robustness and efficiency of the proposed methodology, underscoring its potential for assessing ship rolling response and seakeeping performance under dynamic and uncertain maritime conditions.

## 1. Introduction

A safety and reliability-based design of ships relies on approximate yet physically consistent models of their response to random sea states. In practice, this means representing the vessel as a six-degree-of-freedom dynamical system subjected to stochastic wave loads, with motions in surge, sway, heave, roll, pitch, and yaw (Fig. 1). Among these, intact stability and the risk of capsizing are most directly governed by the roll motion. Consequently, reliably estimating ship roll in random seas is a central requirement in both design and assessment of seakeeping performance (e.g., [1–5]). In realistic seas, the roll excitation is highly irregular and the system response is nonlinear, owing to nonlinearities in both roll damping and restoring. As a result, purely hydrostatic or quasi-static intact-stability criteria cannot capture the relevant dynamics or the likelihood of extreme events. This has prompted a shift toward probabilistic and dynamics-based frameworks that treat roll as a stochastic process driven by random waves and aim to quantify response probability density functions, extreme roll angles, and capsizing probabilities (e.g., [1,2,6]).

Early work on stochastic ship rolling treated the problem as a nonlinear oscillator driven by irregular seas and sought probabilistic descriptions of its response. In this setting, Roberts [7] formulated a stochastic theory for nonlinear ship rolling in irregular seas, using approximate solutions of the associated Fokker–Planck equation to obtain roll response statistics and capsizing probabilities. Related probabilistic methods were later developed to estimate the response distributions and first-passage probabilities for nonlinear roll in random beam seas [8,9]. Within this reliability-oriented context, To and Chen [10] proposed a finite difference method for

*E-mail address:* I.Mitseas@leeds.ac.uk.

https://doi.org/10.1016/j.ymssp.2026.114082
Received 4 December 2025; Received in revised form 6 February 2026; Accepted 24 February 2026
Available online 28 February 2026

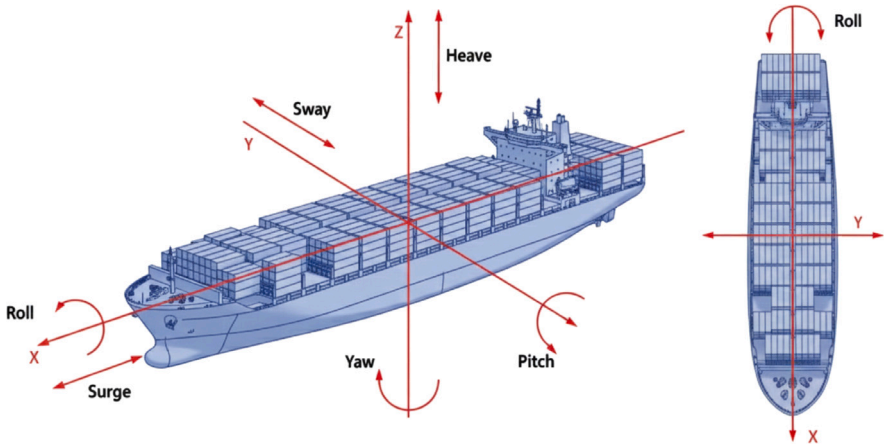


**Fig. 1.** Kinematics of a ship model: Representation of the six degrees of freedom.

efficiently approximating first-passage probabilities of nonlinear ship rolling under non-stationary narrow-band excitation. Building on these foundations, more recent contributions have focused on directly solving the governing Fokker–Planck equation, either through numerical path integration or finite-element discretizations. In particular, path-integration and numerical path-integral schemes have been applied to nonlinear roll under noise excitation, including softening Duffing-type models and systems with inelastic impacts, to compute time-dependent probability density functions, crossing rates, and capsizing probabilities [1,6,11–13], while finite-element formulations of the Fokker–Planck equation have been used to obtain the PDFs for nonlinear random ship rolling and to benchmark Monte Carlo simulations [14].

Complementary to direct Fokker–Planck approaches, a large body of work has employed stochastic averaging and Markov modeling to reduce the roll dynamics to lower-dimensional diffusion processes. Roberts and Vasta [15] introduced a Markov model for the roll energy envelope, enabling efficient estimation of stationary and transient roll statistics from an underlying nonlinear roll equation. Subsequent studies extended stochastic averaging to coupled roll-pitch and roll-heave motions and to more realistic excitation models, including narrow-band and parametric seas (e.g., [16]). More recently, stochastic averaging has been combined with statistical linearization and semi-analytical techniques to study stochastic parametric roll and oblique-wave excitation, providing closed-form or semi-analytical expressions for roll PDFs and capsizing probabilities that compare favorably with numerical path-integration results [17,18].

In parallel with these probabilistic developments, there has been growing interest in more sophisticated mathematical models of response dynamics based on fractional calculus [19–22]. Among classical integer-order modeling approaches, the softening Duffing oscillator has gained considerable traction in the field of ship dynamics, providing a practical approximation of the restoring moment through a linear-plus-cubic formulation (e.g., [4–6,23,24]). While such models are often phenomenological and generally tuned to reproduce key features of the roll response, they typically capture only the most basic aspects of the underlying restoring characteristics. This limitation has motivated the exploration of more expressive formulations. In this regard, fractional-order operators provide a compact way to represent frequency-dependent damping and hydrodynamic memory effects, and have already been successfully applied in diverse areas of engineering such as viscoelasticity, diffusion processes, structural dynamics, and control systems [25–32]. More recently, sophisticated analytical procedures have been developed for the non-stationary stochastic analysis of nonlinear systems with fractional-order terms, leveraging techniques such as path integration [33] and extended statistical linearization [34]. In the context of modeling ship rolling, Spyrou et al. [20] introduced a rudimentary fractional-order deterministic model in which a single fractional derivative term was used to represent the wave-radiation memory kernel in an efficient manner. Building on this idea, Xing and McCue [35] proposed a nonlinear fractional differential equation for roll motion and employed neural-network-based identification to estimate its parameters from experimental data, demonstrating that fractional-order models can reproduce measured roll responses more robustly than conventional integer-order formulations.

To enhance safety margins and support robust analysis and design practice, there is a clear need for analytical and numerical tools that can reproduce ship motions in irregular sea states and quantify the associated risks (e.g., [10,36,37]). Recent advances have moved in this direction by combining nonlinear roll models with softening and hardening restoring characteristics and nonlinear hydrodynamic damping with stochastic process theory and sea-state descriptions consistent with contemporary design standards, such as JONSWAP-type spectra for wave excitation (e.g., [38]). At the same time, fractional calculus-based models in the field have so far been developed mostly in deterministic settings (e.g., [20,35]), whereas stochastic roll dynamics studies based on stochastic averaging, Markov models, or Fokker–Planck and path-integration methods predominantly rely on integer-order formulations with low-order restoring and damping polynomials. The present work aims to bridge these two strands by developing a stochastic fractional-order modeling framework for ship rolling dynamics that incorporates a quintic representation of the restoring moment (capturing both softening and hardening behavior) and a fractional damping term to account for hydrodynamic memory effects, thereby embedding fractional modeling within a stochastic description of nonlinear ship rolling in irregular seas.

The remainder of the paper is organized as follows. Sections 2.1 to 2.5 present the mathematical foundations underpinning the developed fractional-order stochastic roll dynamics framework. Section 2.6 provides insights into the key characteristics and practical implications of the methodology. Section 3 illustrates the framework's application through representative case studies in naval engineering. The accuracy of the proposed technique is evaluated by comparing the derived results with pertinent MCS data obtained from nonlinear ship rolling time–history analysis (RHA). Finally, Section 4 summarizes the main findings and conclusions of the study.

## 2. Mathematical formulation

This section presents the mathematical foundations of the proposed efficient fractional-order stochastic roll dynamics framework. The focus is on the modeling assumptions and simplifying steps that enable numerical efficiency, while remaining fully consistent with the underlying nonlinear governing equation for ship rolling systems endowed with fractional derivative elements.

### 2.1. Non-stationary sea-wave excitation spectrum model

The roll excitation due to sea waves is modeled as a zero-mean, Gaussian, non-stationary stochastic process described in terms of an evolutionary power spectrum (EPS). In this framework, the time-varying distribution of energy across frequencies and time is represented by

$$S_w(\omega,t) = |g(t)|^2\,|F_{\text{roll}}(\omega)|^2\,S_{\text{JS}}(\omega,H_s,T_p) \tag{1}$$

where $S_{\text{JS}}(\omega,H_s,T_p)$ is a stationary JONSWAP-type wave spectrum, $F_{\text{roll}}(\omega)$ is a frequency-dependent transfer function that maps wave energy into roll-moment excitation (e.g., [39]), and $g(t)$ is a deterministic amplitude envelope that drives the non-stationarity in time.

The JONSWAP spectrum [40] is adopted, yielding a narrow-banded energy distribution with an enhanced peak around the dominant wave frequency. In the present formulation, the JONSWAP spectrum is written as

$$S_{\text{JS}}(\omega,H_s,T_p) = 0.3125\,T_p\,H_s^2\left(\frac{\omega}{\omega_p}\right)^{-5}\exp\left[-1.25\left(\frac{\omega}{\omega_p}\right)^{-4}\right]M(\omega) \tag{2}$$

with peak frequency $\omega_p = 2\pi/T_p$ and spectral peak enhancement factor

$$M(\omega) = \left(1-0.287\log\gamma\right)\gamma^{\exp\left[-0.5\left(\frac{\omega/\omega_p-1}{\sigma}\right)^2\right]} \tag{3}$$

The peak-shape parameter is taken as $\gamma = 3.3$, while the width parameter $\sigma$ is set to 0.07 for $\omega < \omega_p$ and 0.09 for $\omega \geq \omega_p$ (e.g., [41]). The mapping from wave elevation to roll-moment excitation is captured through the transfer function $F_{\text{roll}}(\omega)$, here specified in quadratic form as $\left|F_{\text{roll}}(\omega)\right|^2 = C\,\omega^4$ with $C = 3$ reflecting beam-sea loading and system characteristics (e.g., [6,42]). This transfer function broadens the effective excitation spectrum relative to the underlying JONSWAP shape by injecting additional energy into higher frequency components. To introduce non-stationarity, the time envelope $g(t)$ is chosen as

$$g(t) = \left\{0.2 + 0.8\left[\frac{t}{a_t}\exp\left(1-\frac{t}{a_t}\right)\right]^{b_t}\right\}^{1/2} \tag{4}$$

where $a_t$ and $b_t$ control the growth and decay characteristics of the sea state (e.g., [43]). This functional form produces an initially developing sea state, followed by a period of pronounced activity and subsequent attenuation, thereby inducing a stationary-non-stationary-stationary pattern in the excitation.

The peak period $T_p$ and significant wave height $H_s$ are specified in the numerical application section. For illustration, two representative EPS realizations are shown in Fig. 2 for distinct sea-state parameters. In both cases, the underlying JONSWAP spectrum exhibits the characteristic narrow-band peak at the dominant frequency, while the inclusion of $F_{\text{roll}}(\omega)$ is responsible for the observed broadening and elevated energy levels in the high-frequency tail of the excitation spectrum.

### 2.2. Nonlinear ship rolling fractional-order dynamics modeling

The ship rolling motion under stochastic sea-wave excitation is modeled by a second-order fractional differential equation that incorporates a nonlinear restoring moment together with a non-conventional hydrodynamic damping with memory characteristics. Fractional differential equations have recently gained traction in ship-roll modeling (e.g., [5,20,35,44,45]). While the restoring moment is commonly approximated using odd-order polynomials, hydrodynamic damping formulations vary widely across the literature (e.g., [2,5,14,20,35,43–48]). In the herein study, the ship roll motion is modeled using a quintic polynomial representation for the righting arm ($GZ$) curve, combined with a fractional-order hydrodynamic damping scheme (e.g., [20,35]). The proposed governing dynamics nonlinear ship rolling fractional differential equation (FDE) is expressed as

$$(I_{xx}+\delta I_{xx})\,\ddot{\phi}(t) + B\,D_{0,t}^{\alpha}\phi(t) + \Delta\left(C_1\phi(t)+C_3\phi^3(t)+C_5\phi^5(t)\right) = I_{xx}\,w(t) \tag{5}$$

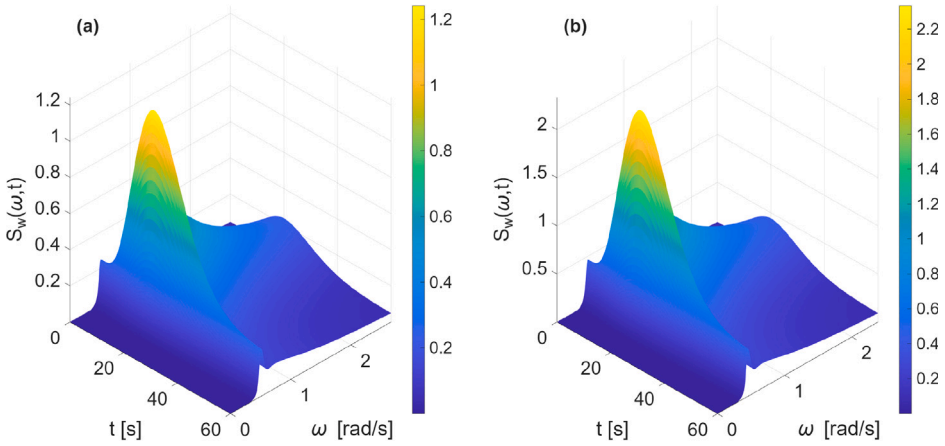


**Fig. 2.** Non-stationary roll-moment excitation spectra $S_{ww}(\omega,t)$ for (a) significant wave height $H_s = 4$ m and peak period $T_p = 12.5$ s, and (b) significant wave height $H_s = 6.5$ m and peak period $T_p = 14.0$ s.

with

$$D^{\alpha}_{0,t}\phi(t) = \frac{1}{\Gamma(1-\alpha)}\int_0^t \frac{\dot{\phi}(\tau)}{(t-\tau)^{\alpha}}\,d\tau, \qquad 0<\alpha<1 \tag{6}$$

denoting a Caputo fractional derivative. In this formulation, $\phi(t)$ denotes the roll angle, $I_{xx}$ is the ship roll moment of inertia, and $\delta I_{xx}$ represents the corresponding added inertia. The term $w(t)$ is a zero-mean, non-stationary Gaussian excitation process characterized by the evolutionary power spectrum given in Eq. (1). The parameters $\Delta$ and $B$ denote the weight displacement and the fractional damping coefficient, respectively. The restoring-moment coefficients $C_1$, $C_3$, and $C_5$ represent the linear, cubic, and quintic contributions extracted from the ship's $GZ$ curve, and are expressed as follows:

$$C_1 = \frac{d(GZ)}{d\phi} = GM \tag{7}$$

$$C_3 = \frac{4}{\phi_v^4}(3A_{\phi v} - GM\phi_v^2) \tag{8}$$

$$C_5 = -\frac{3}{\phi_v^6}(4A_{\phi v} - GM\phi_v^2) \tag{9}$$

In these relations, $GM$ is the metacentric height, $\phi_v$ denotes the vanishing stability angle, and $A_{\phi_v}$ represents the area enclosed by the $GZ$ curve up to $\phi_v$. After dividing by $I_{xx}+\delta I_{xx}$ and inserting the definitions of $C_1$, $C_3$, and $C_5$, Eq. (5) can be rewritten in a form that highlights the influence of all the considered terms in the subsequent stochastic response analysis. Each contribution is multiplied by its own weighting factors, $\varepsilon_1$, $\varepsilon_2$, and $\varepsilon_3$, leading to the final formulation

$$\ddot{\phi}(t) + \varepsilon_1\, b_{\alpha}\, D^{\alpha}_{0,t}\phi(t) + \omega_{\phi}^2\,\phi(t) + \varepsilon_2\, m_3\,\phi^3(t) + \varepsilon_3\, m_5\,\phi^5(t) = \lambda\, w(t) \tag{10}$$

where the corresponding normalized coefficients are defined as

$$\omega_{\phi}^2 = \frac{\Delta GM}{I_{xx}+\delta I_{xx}} \tag{11}$$

$$m_3 = \frac{4\omega_{\phi}^2}{\phi_v^2}\left(\frac{3A_{\phi_v}}{GM\phi_v^2} - 1\right) \tag{12}$$

$$m_5 = -\frac{3\omega_{\phi}^2}{\phi_v^4}\left(\frac{4A_{\phi v}}{GM\phi_v^2} - 1\right) \tag{13}$$

$$b_{\alpha} = \frac{B}{I_{xx}+\delta I_{xx}} \tag{14}$$

and the nondimensional inertia term is defined as $\lambda = \dfrac{I_{xx}}{I_{xx}+\delta I_{xx}}$. The weighting factors provide additional modeling flexibility by allowing the formulation to represent physically realistic hydrodynamic damping and restoring characteristics. This enhances the adaptability of the model, enabling it to capture a broad spectrum of ship-specific dynamic behaviors. Fig. 3 presents representative time histories of ship roll motion under stochastic wave excitation, shown together with the quintic roll restoring lever ($GZ$) curve. The $GZ$ curve, plotted on the left, characterizes the vessel restoring behavior, with the angle of vanishing stability $\phi_v$ indicating the limit beyond which stability becomes uncertain. Exceeding $\phi_v$ does not necessarily lead to capsizing, particularly when higher-order

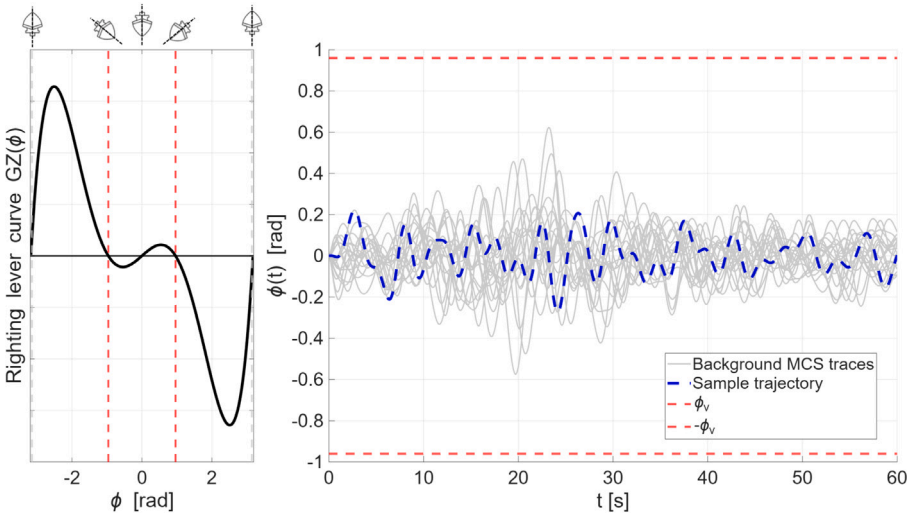


**Fig. 3.** Typical roll restoring arm ($GZ$) curve, characteristic of nonlinear ship dynamics is presented together with ship rolling time-histories under stochastic sea-wave excitation, with $\phi(t) \in [-\phi_v, \phi_v]$ reflecting reliable seakeeping performance without capsizing failures.

restoring effects (for example, a positive fifth-order stiffness term representing restabilizing mechanisms associated with bilge keels or stabilizer fins) generate sufficient righting moment to oppose rollover. Overall, ship stability is governed by a subtle interplay between nonlinear restoring forces and the stochastic nature of the external excitation.

### *2.3. Statistical linearization and stochastic averaging treatment*

With the stochastic excitation process and the nonlinear roll-motion FDE defined, this subsection focuses on the analysis of the system response; see also [49,50]. The adopted framework is based on a stochastic averaging procedure applied to the system dynamics, whereby the original nonlinear second-order FDE is reduced to a first-order stochastic differential equation (SDE) governing the evolution of the roll amplitude. Assuming that the system of Eq. (10) is lightly damped and subjected to the excitation of Eq. (1), it is expected, under non-capsizing conditions, to exhibit a pseudo-harmonic response. This response can be described in terms of a slowly time-varying roll angle amplitude $A(t)$ and a slowly time-varying phase $\theta(t)$. Accordingly, the roll angle and its derivative are approximated as

$$\phi(t) = A(t)\cos(\psi), \quad \dot{\phi}(t) = -\omega(A)A(t)\sin(\psi) \tag{15}$$

where $\psi$ is defined as

$$\psi = \omega(A)t + \theta(t) \tag{16}$$

Here, $A(t)$ and $\theta(t)$ are treated as slowly varying functions of time, and thus may be considered approximately constant over a single oscillation cycle. The time-varying roll angle amplitude $A(t)$ and phase $\theta(t)$ are expressed as

$$A^2(t) = \phi^2(t) + \left(\frac{\dot{\phi}(t)}{\omega(A)}\right)^2 \tag{17}$$

$$\theta(t) = -\omega(A)\,t - \tan^{-1}\left(\frac{\dot{\phi}(t)}{\omega(A)\,\phi(t)}\right) \tag{18}$$

Next, Eq. (10) is equivalently recast in the form

$$\ddot{\phi}(t) + \beta_0\,\dot{\phi}(t) + h\left(t, \phi, D^{\alpha}_{0,t}\phi, \dot{\phi}\right) = \lambda\, w(t) \tag{19}$$

where

$$h\left(t, \phi, D^{\alpha}_{0,t}\phi, \dot{\phi}\right) = \varepsilon_1\, b_\alpha\, D^{\alpha}_{0,t}\phi(t) + z_{\text{roll}}\left(t, \phi\right) - \beta_0\,\dot{\phi}(t) \tag{20}$$

and the nonlinear ship restoring law is given by

$$z_{\text{roll}}\left(t, \phi\right) = \omega_\phi^2\,\phi(t) + \varepsilon_2\, m_3\,\phi^3(t) + \varepsilon_3\, m_5\,\phi^5(t) \tag{21}$$

Here, the linear damping coefficient is $\beta_0 = 2\zeta_0\omega_\phi$, where $\omega_\phi$ denotes the natural frequency of the associated linear system and $\zeta_0$ its critical damping ratio. An equivalent linear system is introduced in the form

$$\ddot{\phi}(t) + \left[\beta_0 + \beta(A)\right]\dot{\phi}(t) + \omega^2(A)\,\phi(t) = \lambda\, w(t) \tag{22}$$

in which $\beta(A)$ and $\omega(A)$ are amplitude-dependent equivalent damping and stiffness coefficients, respectively. By minimizing, in the mean-square sense, the modeling error between Eqs. (19) and (22), one obtains the following expressions for $\beta(A)$ and $\omega^2(A)$:

$$\beta(A) = -\frac{1}{\pi A\,\omega(A)}\left[\int_0^{2\pi} z_{\text{roll}}\big(A\cos\psi\big)\,\sin\psi\,\mathrm{d}\psi + \varepsilon_1\, b_\alpha \int_0^{2\pi} D^{\alpha}_{0,t}\big(A\cos\psi\big)\,\sin\psi\,\mathrm{d}\psi + \pi\,\beta_0\,A\,\omega(A)\right] \tag{23}$$

and

$$\omega^2(A) = \frac{1}{\pi A}\left[\int_0^{2\pi} z_{\text{roll}}\big(A\cos\psi\big)\,\cos\psi\,\mathrm{d}\psi + \varepsilon_1\, b_\alpha \int_0^{2\pi} D^{\alpha}_{0,t}\big(A\cos\psi\big)\,\cos\psi\,\mathrm{d}\psi\right] \tag{24}$$

The expressions in Eqs. (23) and (24) can be further simplified by introducing suitable approximations for the fractional derivative terms, following the methodology outlined in [28,51,52]. In this context, Eq. (23) can be rewritten as

$$\beta(A) = \frac{S(A)}{A\,\omega(A)} + \varepsilon_1\, b_\alpha\,\omega^{\alpha-1}(A)\,\sin\Big(\frac{\alpha\pi}{2}\Big) - \beta_0 \tag{25}$$

and Eq. (24) takes the form

$$\omega^2(A) = \frac{F(A)}{A} + \varepsilon_1\, b_\alpha\,\omega^{\alpha}(A)\,\cos\Big(\frac{\alpha\pi}{2}\Big) \tag{26}$$

where

$$S(A) = -\frac{1}{\pi}\int_0^{2\pi}\Big[\omega_\phi^2 A\cos\psi + \varepsilon_2 m_3 A^3\cos^3\psi + \varepsilon_3 m_5 A^5\cos^5\psi\Big]\,\sin\psi\,\mathrm{d}\psi \tag{27}$$

and

$$F(A) = \frac{1}{\pi}\int_0^{2\pi}\Big[\omega_\phi^2 A\cos\psi + \varepsilon_2 m_3 A^3\cos^3\psi + \varepsilon_3 m_5 A^5\cos^5\psi\Big]\,\cos\psi\,\mathrm{d}\psi \tag{28}$$

By manipulating Eqs. (25)–(28), one arrives at the following semi-analytical expressions for the amplitude-dependent equivalent coefficients:

$$\beta(A) = \varepsilon_1\, b_\alpha\,\omega^{\alpha-1}(A)\,\sin\Big(\frac{\alpha\pi}{2}\Big) - \beta_0 \tag{29}$$

and

$$\omega^2(A) = \omega_\phi^2 + \frac{3}{4}\,\varepsilon_2 m_3 A^2 + \frac{5}{8}\,\varepsilon_3 m_5 A^4 + \varepsilon_1 b_\alpha\,\omega^{\alpha}(A)\cos\Big(\frac{\alpha\pi}{2}\Big) \tag{30}$$

The associated Fokker–Planck partial differential equation (PDE), governing the temporal evolution of the probability density function (PDF) of the response amplitude $A(t)$, is obtained in the form

$$\frac{\partial p(A,t)}{\partial t} = -\left\{\Big[\frac{1}{2}\,\beta_0 + \beta(A)\Big]\,A - \frac{\beta_0\,\omega_\phi^2}{2A\,\omega^2(A)}\right\}\frac{\partial p(A,t)}{\partial A} + \left[\frac{\beta_0\,\omega_\phi^2}{2\,\omega^2(A)}\right]\frac{\partial^2 p(A,t)}{\partial A^2}. \tag{31}$$

### 2.4. Equivalent linearized time-varying stiffness and damping coefficients

Next, an alternative time-varying equivalent linear system to Eq. (22) can be introduced as

$$\ddot{\phi}(t) + \big[\beta_0 + \beta_{\text{eq}}(t)\big]\dot{\phi}(t) + \omega_{\text{eq}}^2(t)\,\phi(t) = \lambda\,w(t) \tag{32}$$

featuring time-varying equivalent elements of the form (e.g., [43,53])

$$\beta_{\text{eq}}(t) = E[\beta(A)], \quad \omega_{\text{eq}}^2(t) = E[\omega^2(A)] \tag{33}$$

which by taking into consideration Eqs. (25) and (26) yield

$$\beta_{\text{eq}}(t) = -\beta_0 + \int_0^{\infty}\frac{S(A)}{A\,\omega(A)}\,p(A,t)\,\mathrm{d}A + \varepsilon_1\, b_\alpha\,\sin\Big(\frac{\alpha\pi}{2}\Big)\int_0^{\infty}\omega^{\alpha-1}(A)\,p(A,t)\,\mathrm{d}A \tag{34}$$

and

$$\omega_{\text{eq}}^2(t) = \int_0^{\infty}\frac{F(A)}{A}\,p(A,t)\,\mathrm{d}A + \varepsilon_1\, b_\alpha\,\cos\Big(\frac{\alpha\pi}{2}\Big)\int_0^{\infty}\omega^{\alpha}(A)\,p(A,t)\,\mathrm{d}A \tag{35}$$

where a tailored form for the non-stationary roll angle amplitude PDF $p(A,t)$ is employed (e.g., [28])

$$p(A,t) = \sin\left(\frac{\alpha\pi}{2}\right) \frac{A\omega_\phi^{\alpha-1}}{c(t)} \exp\left[-\sin\left(\frac{\alpha\pi}{2}\right) \frac{\omega_\phi^{\alpha-1} A^2}{2\,c(t)}\right] \tag{36}$$

with $c(t)$ being a time-varying coefficient to be determined. Elaborating on Eqs. (34) and (35) yield the ship-rolling time-dependent equivalent elements

$$\beta_{\text{eq}}(t) = -\beta_0 + \varepsilon_1\, b_\alpha\, \sin\left(\frac{\alpha\pi}{2}\right) \int_0^\infty \omega^{\alpha-1}(A)\, p(A,t)\, \mathrm{d}A \tag{37}$$

and

$$\omega_{\text{eq}}^2(t) = \int_0^\infty \left[\omega_\phi^2 + \tfrac{3}{4}\,\varepsilon_2 m_3 A^2 + \tfrac{5}{8}\,\varepsilon_3 m_5 A^4\right] p(A,t)\,\mathrm{d}A + \varepsilon_1\, b_\alpha\, \cos\left(\frac{\alpha\pi}{2}\right) \int_0^\infty \omega^{\alpha}(A)\, p(A,t)\,\mathrm{d}A \tag{38}$$

which can be further manipulated by considering the PDF of Eq. (36) into

$$\beta_{\text{eq}}(t) = -\beta_0 + \varepsilon_1 b_\alpha\, \sin^2\left(\frac{\alpha\pi}{2}\right) \frac{\omega_\phi^{\alpha-1}}{c(t)}\, I_1\big(c(t)\big) \tag{39}$$

and

$$\omega_{\text{eq}}^2(t) = \sin\left(\frac{\alpha\pi}{2}\right) \frac{\omega_\phi^{\alpha-1}}{c(t)}\, I_2\big(c(t)\big) + \frac{1}{2}\,\varepsilon_1 b_\alpha\, \sin(\alpha\pi)\, \frac{\omega_\phi^{\alpha-1}}{c(t)}\, I_3\big(c(t)\big) \tag{40}$$

where

$$I_1\big(c(t)\big) = \int_0^\infty A\,\omega^{\alpha-1}(A)\, \exp\big[-K(t)A^2\big]\,\mathrm{d}A \tag{41}$$

$$I_2\big(c(t)\big) = \int_0^\infty \left[\omega_\phi^2 + \tfrac{3}{4}\,\varepsilon_2 m_3 A^2 + \tfrac{5}{8}\,\varepsilon_3 m_5 A^4\right] A\, \exp\big[-K(t)A^2\big]\,\mathrm{d}A \tag{42}$$

and

$$I_3\big(c(t)\big) = \int_0^\infty A\,\omega^{\alpha}(A)\, \exp\big[-K(t)A^2\big]\,\mathrm{d}A \tag{43}$$

with

$$K(t) = \frac{\sin\left(\frac{\alpha\pi}{2}\right)\, \omega_\phi^{\alpha-1}}{2\,c(t)} \tag{44}$$

### 2.5. Deterministic and stochastic averaging treatment

For the equivalent linearized system of Eq. (32), Eqs. (15) and (16) become

$$\phi(t) = A(t)\cos(\psi), \quad \dot{\phi}(t) = -\omega_{\text{eq}}(t) A(t)\sin(\psi) \tag{45}$$

where $\psi$ is defined now as

$$\psi = \omega_{\text{eq}}(t)t + \theta(t) \tag{46}$$

leading to

$$A^2(t) = \phi^2(t) + \left(\frac{\dot{\phi}(t)}{\omega_{\text{eq}}(t)}\right)^2 \tag{47}$$

Differentiating Eqs. (45) and considering Eq. (32) yields

$$\dot{A}(t) = -\beta_0\, A(t)\, \sin^2\psi - \beta_{\text{eq}}(t)\, A(t)\, \sin^2\psi - \lambda\, \frac{w(t)\,\sin\psi}{\omega_{\text{eq}}(t)} \tag{48}$$

where $\lambda = \dfrac{I_{xx}}{I_{xx} + \delta I_{xx}}$. A standard averaging approach (e.g., [54]) yields a first-order SDE governing the evolution of roll angle amplitude

$$\dot{A}(t) = -\frac{1}{2}\big[\beta_0 + \beta_{\text{eq}}(t)\big]\, A(t) + \frac{\pi\,\lambda^2\, S_w\big(\omega_{\text{eq}}(t), t\big)}{2\, A(t)\, \omega_{\text{eq}}^2(t)} + \frac{\big[\pi\, S_w\big(\omega_{\text{eq}}(t), t\big)\big]^{1/2}}{\omega_{\text{eq}}(t)}\, \lambda\, \eta(t) \tag{49}$$

where $\eta(t)$ is a zero-mean and delta-correlated process of unit intensity, with $E(\eta(t)) = 0$; and $E(\eta(t)\eta(t+\tau)) = \delta(t)$ (e.g., [49,55,56]). Eq. (49) signifies that the amplitude process $A(t)$ is decoupled from the phase $\theta(t)$ and, thus, can be modeled as an one-dimensional

Markov process, enabling the formulation of a Fokker–Planck equation that governs the associated roll angle amplitude PDF considering the ship-rolling time-dependent equivalent elements (e.g., [54,57])

$$\frac{\partial p(A,t)}{\partial t} = -\frac{\partial}{\partial A}\left\{\left[-\frac{1}{2}\left(\beta_0+\beta_{\text{eq}}(t)\right)A+\frac{\pi\,\lambda^2\,S_w\left(\omega_{\text{eq}}(t),t\right)}{2\,A\omega_{\text{eq}}^2(t)}\right]p(A,t)\right\} + \frac{1}{4}\frac{\partial}{\partial A}\left\{\frac{\pi\,\lambda^2\,S_w\left(\omega_{\text{eq}}(t),t\right)}{\omega_{\text{eq}}^2(t)}\frac{\partial p(A,t)}{\partial A}+\frac{\partial}{\partial A}\left[\frac{\pi\,\lambda^2\,S_w\left(\omega_{\text{eq}}(t),t\right)}{\omega_{\text{eq}}^2(t)}\,p(A,t)\right]\right\} \tag{50}$$

Substituting the PDF of Eq. (36) into Eq. (50), the following nonlinear ordinary differential equation (ODE) can be obtained for the computation of the time-varying coefficient $c(t)$

$$\dot{c}(t) = -\left[\beta_0+\beta_{\text{eq}}(t)\right]c(t)+\lambda^2\,\sin\left(\frac{\alpha\pi}{2}\right)\omega_\phi^{\alpha-1}\,\frac{\pi\,S_w\left(\omega_{\text{eq}}(t),t\right)}{\omega_{\text{eq}}^2(t)} \tag{51}$$

Notably, Eq. (51) can be readily solved at a low computational cost by employing any standard numerical integration scheme, such as the Runge–Kutta.

### 2.6. Discussion on attributes of the proposed stochastic roll dynamics method

This section outlines key attributes of the proposed fractional-order stochastic roll dynamics framework, with emphasis on its advantages, limitations, and practical applicability. Overall, the methodology provides a versatile and computationally efficient tool for assessing response statistics of ship–sea systems that exhibit complex nonlinear dynamic behavior. Direct numerical solution of the underlying fractional differential equation of roll can be computationally demanding, owing to the need to evaluate the convolution integral associated with the fractional derivative operator in the presence of strong nonlinearities. The proposed semi-analytical framework mitigates this difficulty by working at the level of equivalent linearized parameters rather than time-marching the full fractional system.

A central strength of the approach is its ability to represent systems with both softening and hardening restoring nonlinearities, while simultaneously providing a compact representation of hereditary (memory-type) hydrodynamic damping through a fractional-order operator (e.g., [20,35,44,45]). This combined treatment of nonlinear restoring forces and fractional-order damping inevitably increases model complexity, but it substantially improves the framework's ability to capture realistic roll dynamics in non-stationary sea states. In particular, the fractional operator introduces history dependence and frequency-dependent phase lag/dissipation in an economical (low-parameter) manner, offering a reduced-order alternative to high-order integer approximations when modeling radiation-memory effects. It is also worth noting that the fractional operator in Eq. (6) is defined for $0 < \alpha < 1$; nevertheless, increasing $\alpha$ provides a continuous transition toward more local-in-time damping behavior, approached in the limiting sense as $\alpha \to 1^-$. Accordingly, varying $\alpha$ offers a convenient means to quantify the influence of memory on the non-stationary roll response, with smaller $\alpha$ implying a more pronounced nonlocal-in-time (hereditary) character and $\alpha \to 1^-$ approaching local-in-time behavior.

By relying on statistical linearization under a pseudo-harmonic assumption, the method accounts for amplitude- and time-dependent variations in the equivalent natural frequency and damping, while retaining analytical tractability. This makes it well suited to tracking and quantifying moving resonance phenomena (e.g., [56,58]), where relatively small changes in excitation or system properties can lead to pronounced response amplification. At the same time, the framework imposes relatively mild requirements on the excitation model: it only assumes that the input is Gaussian. As a result, it can be applied across a broad spectrum of sea states, including non-stationary conditions in which wave intensity and spectral characteristics evolve over time.

The approach does, however, inherit certain limitations. The combination of stochastic averaging and statistical linearization is most reliable for lightly or moderately nonlinear systems. Its accuracy may deteriorate in heavily damped configurations or in the presence of very strong nonlinearities, as reported in the broader random-vibration literature (e.g., [59,60]). In such regimes, higher-order corrections or fully numerical methods may be required to maintain predictive fidelity.

In the context of ship rolling, hydrodynamic radiation effects are classically represented in the time domain through Cummins-type formulations, where memory is captured by a convolution (retardation) integral acting on the past velocity history. From this perspective, fractional-order models are most appropriately viewed as compact surrogate representations of such hereditary radiation-memory behavior, rather than as introducing fundamentally new hydrodynamic physics (e.g., [61]). In this setting, one frequently proposed interpretation of a fractional derivative of order greater than one is that it blends added hydrodynamic inertia and potential (radiation) damping into a single operator; however, this interpretation remains largely heuristic because added inertia and damping cannot be explicitly disentangled from the identified fractional coefficients (e.g., [20,35,44,61]). This motivates the modeling choice adopted here: added inertia and damping are represented transparently as distinct contributions in the roll equation (Eq. (10)), with the added moment of inertia $\delta I_{xx}$ introduced explicitly as a constant term, consistent with common seakeeping practice (e.g., [46]), while the fractional operator is restricted to orders between 0 and 1 so that it acts solely as a memory-type damping surrogate. Notably, fractional-order models have demonstrated superior fitting capabilities for roll response data (e.g., [35]), as well as strong representation capabilities across a wide range of engineering applications [21,25–27,29–32]. In this way, the proposed framework retains the identification and fitting flexibility of fractional-order models, while remaining consistent with established hydrodynamic modeling practice through a transparent representation of inertial properties and radiation-memory effects.

In summary, the proposed method provides a flexible, physically interpretable, and computationally tractable framework for response analysis under non-stationary sea-wave excitation. By combining evolutionary excitation modeling, nonlinear restoring behavior, and fractional damping within a unified semi-analytical scheme, it aligns well with practical needs in naval engineering for efficient yet sophisticated modeling of nonlinear ship rolling dynamics.

## 3. Numerical application

This section presents numerical results for the proposed fractional-order modeling framework for nonlinear ship rolling, based on the developments of Sections 2.1 to 2.5. Variations in the input significant wave height $H_s$, peak period $T_p$, system weighting factors $\varepsilon_1$, $\varepsilon_2$, and $\varepsilon_3$, as well as the fractional derivative order $\alpha$ are considered. The results are validated against pertinent MCS data to demonstrate the efficiency and reliability of the proposed approach. The reference ship is characterized by vanishing stability angle $\phi_v = 0.96$ rad, area under the righting-arm curve up to this angle $A_{\phi v} = 0.67$ m rad, metacentric height $GM = 3$ m, roll moment of inertia $I_{xx} = 1 \times 10^8$ kg m$^2$, added inertia $\delta I_{xx} = 0.2 I_{xx}$, displacement $\Delta = 1 \times 10^8$ N and fractional damping constant $B = 7 \times 10^8$ N m s (e.g., [62,63]). Lastly, the restoring arm is represented by a fifth-order polynomial in roll angle, with coefficients chosen in line with realistic $GZ$ curves.

The excitation is specified through the significant wave height $H_s$ and the peak period $T_p$ of the underlying JONSWAP spectrum, and by the envelope parameters $\alpha_t = 20$ and $b_t = 5$ controlling the build-up and decay of sea severity. For all cases, the performance of the proposed stochastic ship dynamics fractional-order methodology is assessed by direct comparison with MCS results based on 10,000 realizations (e.g., [6,53]), demonstrating its capability and robustness in quantifying higher-order rolling statistics under sea-wave non-stationary excitation. More precisely, the spectral representation method outlined in [64] is employed to create the ensemble of realizations, compatible with the reference seed power spectrum corresponding to a specific nominal wave height and peak period for the induced hydrodynamic excitation of Eq. (1). The corresponding system response is then obtained through numerical integration of the governing fractional-order equation of nonlinear ship motion Eq. (10) by resorting to an L1-algorithm (e.g., [65]). In the first set of results (Ship Configuration A), the weighting factors are chosen as $\varepsilon_1 = 1$, $\varepsilon_2 = 1.5$, $\varepsilon_3 = 1$, with a fractional derivative order $\alpha = 0.65$ and a critical damping ratio for the linear damping coefficient $\zeta_0 = 0.03$. These values give a roll model where third-order softening dominates the restoring behavior and the fifth-order term only mildly modifies the curve at larger angles. Fig. 4 shows the non-stationary standard deviation of ship rolling $\sigma_\phi(t)$ along with representative Monte Carlo roll time histories, for two sea states: $H_s = 4$ m (plots a and c) and $H_s = 5.5$ m (plots b and d) with $T_p = 12.5$ s. In both cases the stochastic fractional-order method reproduces very well the build-up, peak, and decay of $\sigma_\phi(t)$ obtained from Monte Carlo simulation. The peak of $\sigma_\phi(t)$ occurs during the interval where the excitation envelope is strongest; before and after this period the curves tend toward lower, nearly constant levels, reflecting the imposed stationary-non-stationary-stationary structure of the sea spectrum. For the milder sea state $H_s = 4$ m, the sample Monte Carlo roll time-histories rarely exceed about 0.3 - 0.4 rad. For $H_s = 5.5$ m the response becomes noticeably stronger, with a clear increase in peak standard deviation, however, the roll angles still remain below the vanishing stability limits $\pm\phi_v$ indicated by the dashed red lines. In both sea states, the Monte Carlo trajectories show no capsizing events over the simulated time horizon, supporting the interpretation of these cases as reliable but noticeably nonlinear seakeeping conditions. Figs. 5 and 6 provide the non-stationary roll amplitude probability density surfaces. For very small times near $t = 0$ s the roll motion is initiated from rest, so the amplitude distribution collapses to a Dirac mass at zero, which appears as a narrow spike. For $H_s = 4$ m, Fig. 5(a) shows the non-stationary amplitude PDF surface predicted by the fractional-order method, while Fig. 5(b) shows the corresponding surface reconstructed from the Monte Carlo ensemble (10,000 realizations). The two surfaces are very similar: both begin with a narrow, high-peaked ridge at small amplitudes, broaden during the strongly excited phase, and gradually shrink again as the excitation envelope decays. This behavior reflects the inheritance of the stationary-non-stationary-stationary pattern of the wave input by the roll response. Fig. 5(c) and (d) present cuts through these surfaces at selected times $t = 5, 20, 35, 50$ s. At each time, the method amplitude PDFs agree closely with estimates from Monte Carlo, including the shift of the mode to larger amplitudes during the most energetic phase. The same trends are observed for the higher sea state $H_s = 5.5$ m in Fig. 6. The amplitude PDFs are wider and have heavier right tails, consistent with a higher probability of larger roll amplitudes, but the agreement between the fractional-order method and Monte Carlo remains good across time and amplitude.

In the second set of results (Ship Configuration B) the weighting factors are changed to $\varepsilon_1 = 1$, $\varepsilon_2 = 1.5$, $\varepsilon_3 = 1.5$, and the fractional derivative order is set equal to $\alpha = 0.70$. The peak period is now $T_p = 14$ s. Fig. 7 presents $\sigma_\phi(t)$ and representative time histories for Ship Configuration B at $H_s = 4$ m (plots a and c) and $H_s = 6.5$ m (plots b and d). Again, the fractional-order method follows closely the Monte Carlo standard deviation curves over the entire simulation window, including the initial transient and the subsequent non-stationary peak. For $H_s = 4$ m, the behavior remains qualitatively similar to Ship Configuration A. The stronger sea state and increased nonlinearity produce higher response levels and more pronounced cycle-to-cycle variability in the Monte Carlo histories (case $H_s = 6.5$ m). Still, the fractional-order method captures both the timing and magnitude of the peak $\sigma_\phi(t)$ with good accuracy, and predicts the gradual decay toward a lower stationary variance as the excitation envelope weakens. The representative Monte Carlo trajectories in Fig. 7(d) show several near-critical excursions approaching the vanishing stability angles, but no sustained growth or capsizing over the simulated time. Figs. 8 and 9 show the amplitude PDF surfaces and selected PDF cuts for Ship Configuration B, at $H_s = 4$ m and $H_s = 6.5$ m respectively. The proposed fractional-order method remains in close agreement with Monte Carlo across the time-amplitude plane. For both sea states, the cut-through plots at selected time instants confirm that the method adequately reproduces both the mode and the spread of the amplitude distributions, demonstrating its robustness.

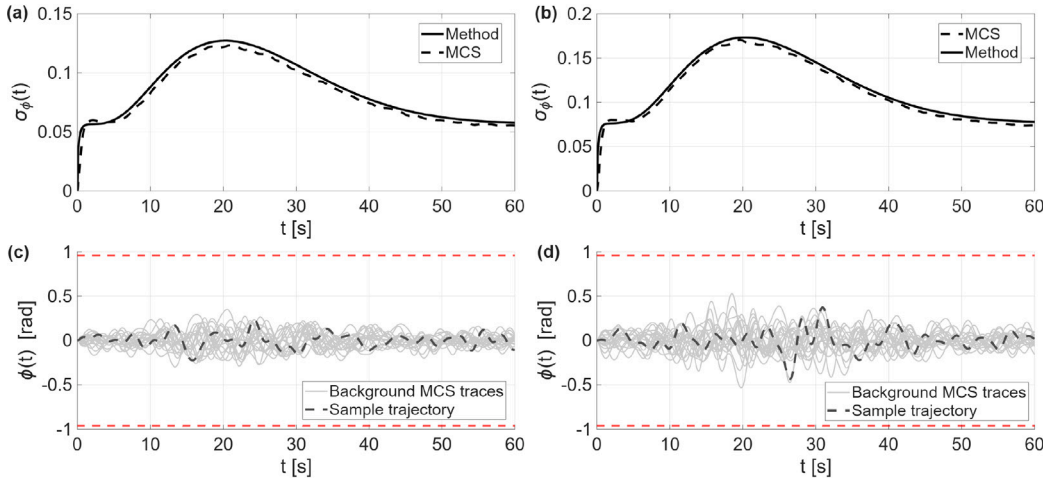


**Fig. 4.** Non-stationary response statistics of a nonlinear ship rolling system under non-stationary sea-wave excitation for nominal wave heights (a) $H_s = 4$ m and (b) $H_s = 5.5$ m with $T_p = 12.5$ s are obtained by the proposed fractional-order method and compared with MCS data (10,000 realizations). Plots (c) and (d) display representative MCS ship rolling time histories; red dashed lines indicate the vanishing-stability roll angles $\pm\phi_v$; system $\varepsilon_1 = 1$, $\varepsilon_2 = 1.5$, $\varepsilon_3 = 1$, $\alpha = 0.65$.

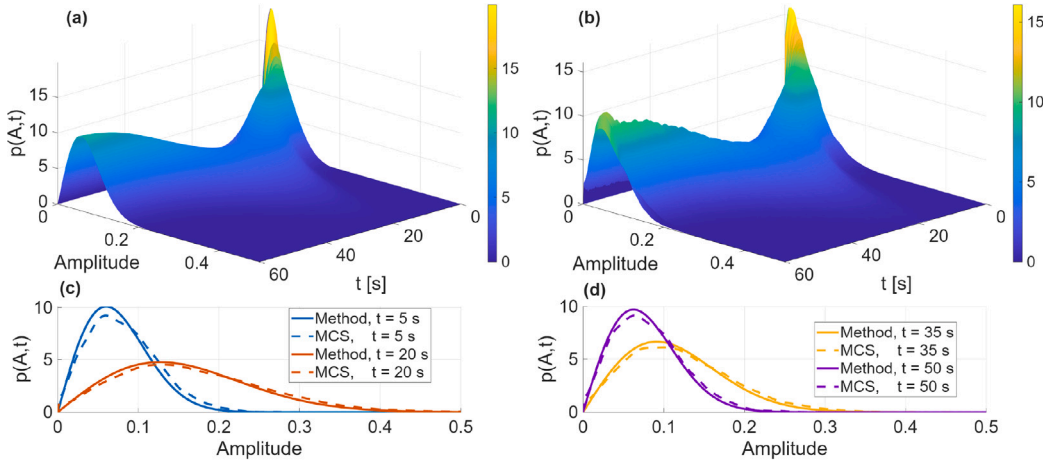


**Fig. 5.** Non-stationary roll amplitude PDF surface obtained by (a) the proposed fractional-order method and compared with (b) MCS data (10,000 realizations) for nominal wave height $H_s = 4$ m and $T_p = 12.5$ s. Plots (c) and (d) present comparison of the method estimates against MCS at selected time instants.

In the third set of results (Ship Configuration C), the weighting factors are kept identical to Ship Configuration A, i.e., $\varepsilon_1 = 1$, $\varepsilon_2 = 1.5$, and $\varepsilon_3 = 1$, while the fractional derivative order is reduced to $\alpha = 0.40$ (with $\zeta_0 = 0.03$). This choice increases the relative contribution of memory-type hydrodynamic damping embedded in the fractional operator, i.e., it strengthens the nonlocal-in-time character of the dissipation mechanism within the admissible range $0 < \alpha < 1$. If $B$ is kept fixed, reducing $\alpha$ generally strengthens the memory effect and (for the present case with $\omega_\phi > 1$) tends to reduce the effective damping around the roll-frequency band, leading to a higher and more persistent $\sigma_\phi(t)$, although strict monotonicity is not guaranteed in the nonlinear non-stationary setting. Figs. 10 to 12 present the corresponding non-stationary response statistics and amplitude probability density surfaces for $H_s = 4$ m and $H_s = 5.5$ m (with the same excitation-envelope parameters as in the previous cases). Comparing Fig. 4 ($\alpha = 0.65$) with Fig. 10 ($\alpha = 0.40$), the time of peak $\sigma_\phi(t)$ remains within the same excitation-dominated interval (shift is marginal), while the post-peak relaxation appears slightly more sustained, which is consistent with the stronger history dependence introduced by reducing $\alpha$. The method exhibits satisfactory agreement with the Monte Carlo benchmarks, tracking the build-up, peak, and decay of $\sigma_\phi(t)$ over the simulation window, while the stronger sea state yields higher response levels and broader amplitude distributions, reflected in heavier right tails of $p(A,t)$. Relative to the baseline $\alpha = 0.65$ case (Ship Configuration A), the smaller order $\alpha = 0.40$ enhances the role of history dependence in the damping, which is reflected in a modified non-stationary variance evolution and the associated time-varying amplitude PDFs.

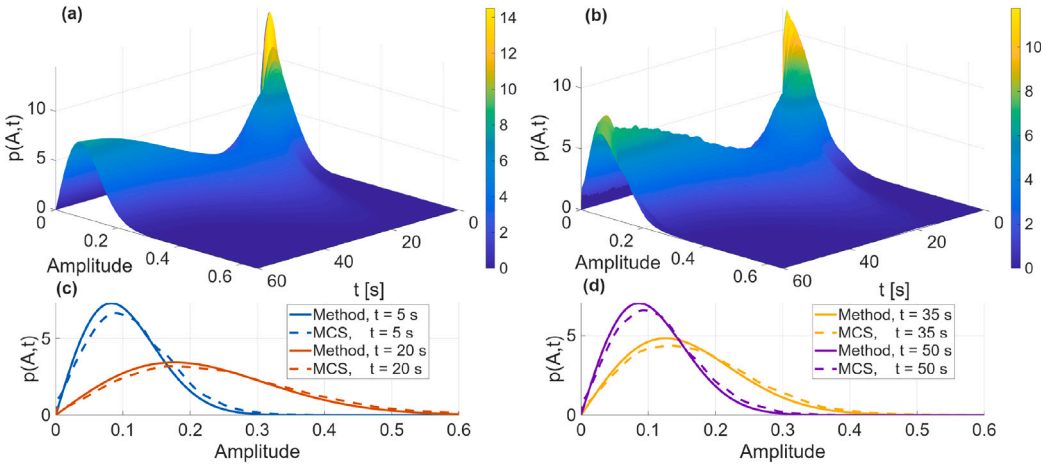


**Fig. 6.** Non-stationary roll amplitude PDF surface obtained by (a) the proposed fractional-order method and compared with (b) MCS data (10,000 realizations) for nominal wave height $H_s = 5.5$ m and $T_p = 12.5$ s. Plots (c) and (d) present comparison of the method estimates against MCS at selected time instants.

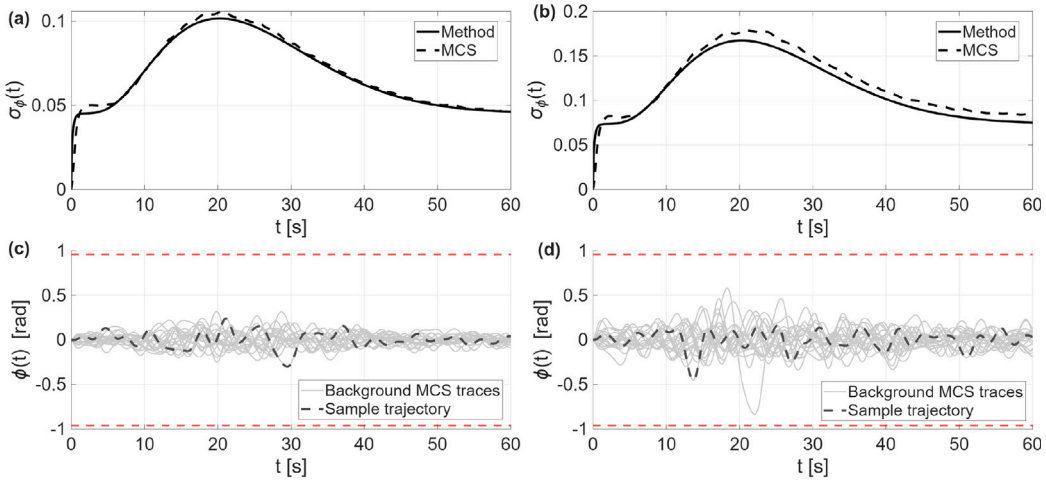


**Fig. 7.** Non-stationary response statistics of a nonlinear ship rolling system under non-stationary sea-wave excitation for nominal wave heights (a) $H_s = 4$ m and (b) $H_s = 6.5$ m with $T_p = 14$ s are obtained by the proposed fractional-order method and compared with MCS data (10,000 realizations). Plots (c) and (d) display representative MCS ship rolling time histories; red dashed lines indicate the vanishing-stability roll angles $\pm\phi_v$; system $\varepsilon_1 = 1$, $\varepsilon_2 = \varepsilon_3 = 1.5$, $\alpha = 0.70$.

It can be observed that, at any given time instant, the proposed methodology exhibits satisfactory agreement with the MCS benchmark across the examined ranges of weighting factors $\varepsilon$ and fractional derivative order $\alpha$. Its consistent performance under different nominal wave heights and peak periods further underscores the robustness of the approach in accommodating a variety of excitation characteristics, making it suitable for application across diverse and representative sea states. In the present case studies, the dominant softening behavior arises primarily from the intrinsic properties of the restoring coefficients: the magnitude of $m_3$ is significantly larger than that of $m_5$, so the third-order softening term governs the nonlinear response. The chosen combinations of $\varepsilon_1$, $\varepsilon_2$, $\varepsilon_3$ and $\alpha$ provide a balanced yet flexible representation of softening and hardening restoring effects, while enabling a realistic description of non-conventional and hereditary hydrodynamic damping through the fractional operator, in line with contemporary ship-roll modeling initiatives. By employing a fifth-order polynomial for the $GZ$ curve and introducing tailored weighting factors together with fractional derivative orders, the method is able to capture both softening and hardening restoring behaviors, as well as complex non-conventional damping with memory effects.

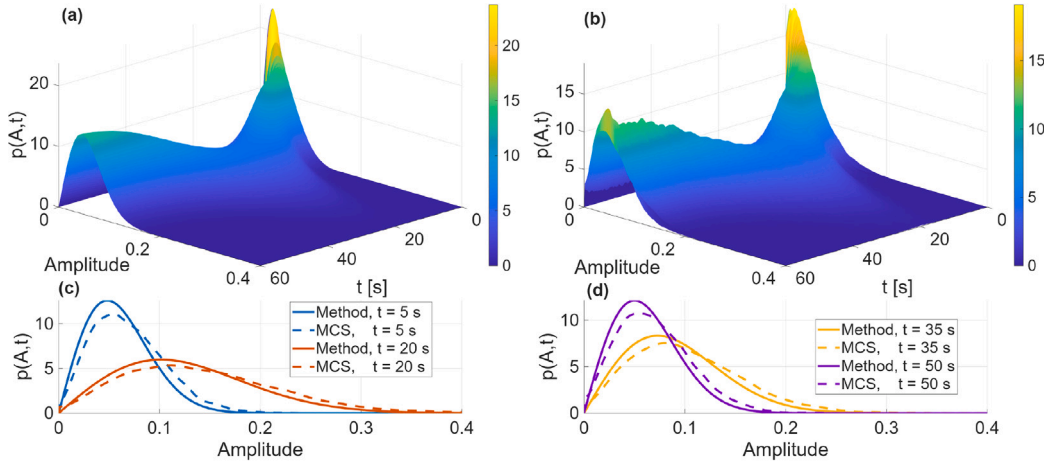


**Fig. 8.** Non-stationary roll amplitude PDF surface obtained by (a) the proposed fractional-order method and compared with (b) MCS data (10,000 realizations) for nominal wave height $H_s = 4$ m and $T_p = 14$ s. Plots (c) and (d) present comparison of the method estimates against MCS at selected time instants.

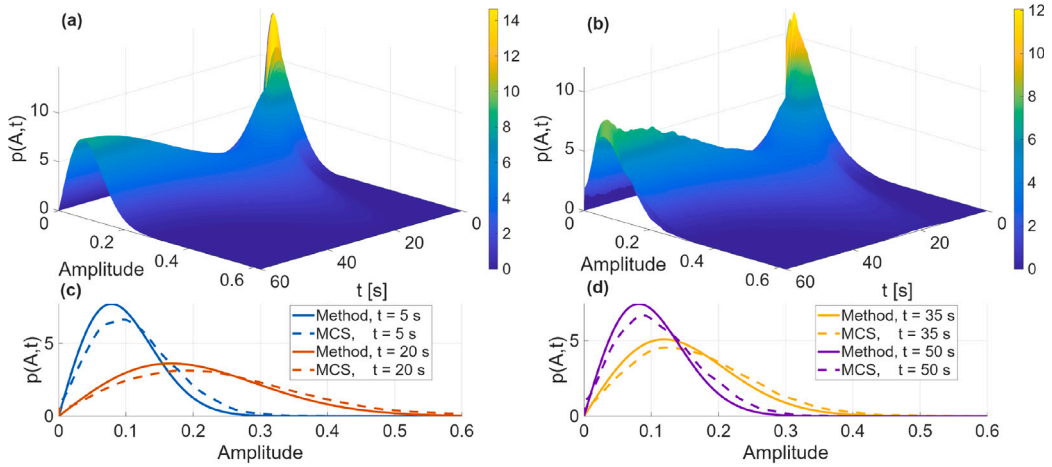


**Fig. 9.** Non-stationary roll amplitude PDF surface obtained by (a) the proposed fractional-order method and compared with (b) MCS data (10,000 realizations) for nominal wave height $H_s = 6.5$ m and $T_p = 14$ s. Plots (c) and (d) present comparison of the method estimates against MCS at selected time instants.

## 4. Concluding remarks

This study proposed an efficient fractional-order stochastic roll dynamics framework for assessing the non-stationary response statistics of ships subjected to stochastic sea-wave excitations. The modeling is grounded in a comprehensive and physically consistent nonlinear formulation, integrating both softening and hardening restoring moment characteristics alongside non-conventional hydrodynamic fractional damping that naturally embeds memory characteristics. Non-stationary sea states with time-varying intensity and spectral content are described through an evolutionary excitation spectrum, enabling a realistic representation of open-sea conditions. Central to the approach is a refined combination of stochastic averaging and statistical linearization, which enables computationally efficient estimation of time-dependent second-order response statistics along with the associated roll angle amplitude probability-density surfaces. Notably, the fractional operator in the damping term plays an important role, as it introduces memory and frequency-dependent dissipation consistent with contemporary ship roll modeling initiatives. An additional benefit of the technique is the by-product determination of equivalent linear, time-dependent stiffness and damping elements. This feature can be particularly useful for tracking and quantifying moving resonance phenomena, which may lead to significant response amplification in nonlinear systems. In this sense, the proposed approach demonstrates computational efficiency and reliable agreement with benchmark Monte Carlo results, while advancing the theoretical and practical toolkit available for modern nonlinear ship rolling dynamic analysis. Overall, the results highlight that the proposed fractional-order framework offers a computationally efficient yet physically rich alternative to large-scale Monte Carlo simulation. By combining evolutionary excitation modeling,

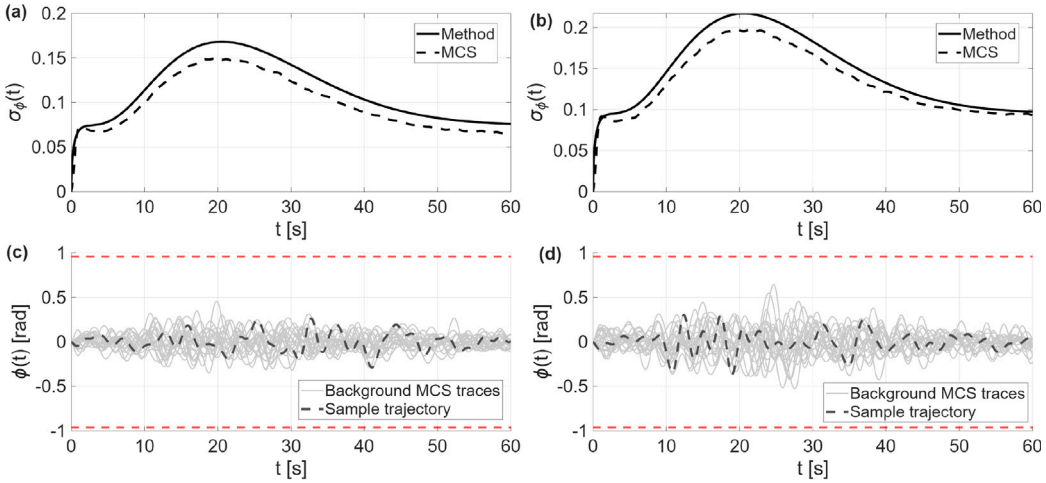


**Fig. 10.** Non-stationary response statistics of a nonlinear ship rolling system under non-stationary sea-wave excitation for nominal wave heights (a) $H_s = 4$ m and (b) $H_s = 5.5$ m with $T_p = 12.5$ s are obtained by the proposed fractional-order method and compared with MCS data (10,000 realizations). Plots (c) and (d) display representative MCS ship rolling time histories; red dashed lines indicate the vanishing-stability roll angles $\pm\phi_v$; system $\varepsilon_1 = 1$, $\varepsilon_2 = 1.5$, $\varepsilon_3 = 1$, $\alpha = 0.40$.

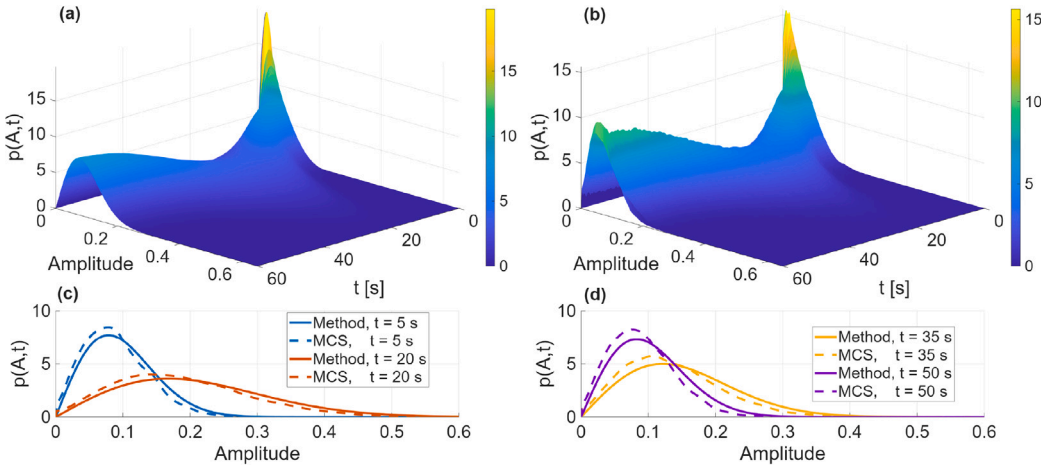


**Fig. 11.** Non-stationary roll amplitude PDF surface obtained by (a) the proposed fractional-order method and compared with (b) MCS data (10,000 realizations) for nominal wave height $H_s = 4$ m and $T_p = 12.5$ s. Plots (c) and (d) present comparison of the method estimates against MCS at selected time instants.

nonlinear restoring, and hereditary fractional damping within a unified semi-analytical scheme, it provides a versatile tool for assessing ship roll response and seakeeping performance under dynamically evolving and uncertain sea conditions.

## Declaration of competing interest

The authors declare that they have no known competing financial interests or personal relationships that could have appeared to influence the work reported in this paper.

## Data availability

Data will be made available on request.

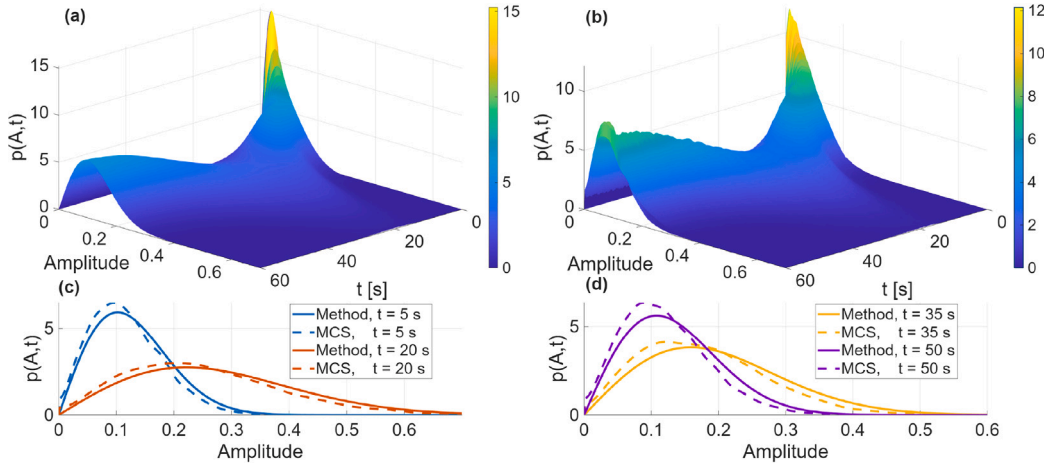


**Fig. 12.** Non-stationary roll amplitude PDF surface obtained by (a) the proposed fractional-order method and compared with (b) MCS data (10,000 realizations) for nominal wave height $H_s = 5.5$ m and $T_p = 12.5$ s. Plots (c) and (d) present comparison of the method estimates against MCS at selected time instants.

## References


[1] W. Chai, A. Naess, B.J. Leira, Stochastic nonlinear ship rolling in random beam seas by the path integration method, Probab. Eng. Mech. 44 (2016) 43–52.
[2] G. Malara, P.D. Spanos, F. Arena, Maximum roll angle estimation of a ship in confused sea waves via a quasi-deterministic approach, Probab. Eng. Mech. 35 (2014) 75–81.
[3] L. Arnold, I. Chueshov, G. Ochs, Stability and capsizing of ships in random sea-a survey, Nonlinear Dynam. 36 (2004) 135–179.
[4] V.L. Belenky, N.B. Sevastianov, Stability and Safety of Ships: Risk of Capsizing, The Society of Naval Architects and Marine Engineers, 2007.
[5] K. Spyrou, J. Thompson, The nonlinear dynamics of ship motions: A field overview and some recent developments, Philos. Trans. R. Soc. A: Math. Phys. Eng. Sci. 358 (2000) 1735–1760.
[6] I.A. Kougioumtzoglou, P.D. Spanos, Stochastic response analysis of the softening Duffing oscillator and ship capsizing probability determination via a numerical path integral approach, Probab. Eng. Mech. 35 (2014) 67–74.
[7] J.B. Roberts, A stochastic theory for nonlinear ship rolling in irregular seas, J. Ship Res. 26 (4) (1982) 229–245.
[8] S.-R. Hsieh, A.W. Troesch, S.W. Shaw, A nonlinear probabilistic method for predicting vessel capsizing in random beam seas, Proc. R. Soc. Lond. Ser. A Math. Phys. Eng. Sci. 446 (1926) (1994) 195–211.
[9] G.-K. Er, V.P. Iu, Probabilistic solutions to nonlinear random ship roll motion, J. Eng. Mech. 125 (5) (1999) 570–574.
[10] C.W.S. To, Z. Chen, First passage time of nonlinear ship rolling in narrow band non-stationary random seas, J. Sound Vib. 309 (2008) 197–209.
[11] A. Jamnongpipatkul, Z. Su, J.M. Falzarano, Nonlinear ship rolling motion subjected to noise excitation, Ocean. Syst. Eng. 1 (3) (2011) 249–261.
[12] Z. Ren, W. Xu, D. Wang, Dynamic and first passage analysis of ship roll motion with inelastic impacts via path integration method, Nonlinear Dynam. 97 (2019) 391–402.
[13] P. Kumar, S. Narayanan, Stochastic roll dynamics of smooth and impacting vessels in random waves, Ocean Eng. (ISSN: 0029-8018) 307 (2024) 118190.
[14] J. Chen, J. Yang, K. Shen, Z. Zheng, Z. Chang, Stochastic dynamic analysis of rolling ship in random wave condition by using finite element method, Ocean Eng. 250 (2022) 110973.
[15] J.B. Roberts, M. Vasta, Markov modelling and stochastic identification for nonlinear ship rolling in random waves, Philos. Trans. R. Soc. Lond. Ser. A Math. Phys. Eng. Sci. 358 (1771) (2000) 1917–1941.
[16] L. Dostal, E.J. Kreuzer, N.S. Namachchivaya, Non-standard stochastic averaging of large-amplitude ship rolling in random seas, Proc. R. Soc. A: Math. Phys. Eng. Sci. 468 (2012) 4146–4173.
[17] W. Chai, L. Dostal, A. Naess, B.J. Leira, A comparative study of the stochastic averaging method and the path integration method for nonlinear ship roll motion in random beam seas, J. Mar. Sci. Technol. 23 (4) (2018) 854–865.
[18] L.-y. Wang, Y.-g. Tang, Y. Li, J.-c. Zhang, L.-q. Liu, Studies on stochastic parametric roll of ship with stochastic averaging method, China Ocean Eng. 34 (2) (2020) 289–298.
[19] J.A.T.M.J. Sabatier, O.P. Agrawal, J.A.T. Machado, Advances in Fractional Calculus, vol. 4, Springer, 2007.
[20] K.J. Spyrou, S. Niotis, C. Panagopoulou, Novel modeling of ship rolling based on fractional calculus, in: Proceedings of the 6th Osaka Colloquium on Seakeeping and Stability of Ships, Osaka, Japan, 2008, pp. 1–8.
[21] I.A. Kougioumtzoglou, P. Ni, I.P. Mitseas, V.C. Fragkoulis, M. Beer, An approximate stochastic dynamics approach for design spectrum-based response analysis of nonlinear oscillators with fractional derivative elements, Int. J. Non-Linear Mech. 146 (2022) 104178.
[22] Y. Zhang, S. Li, F. Kong, Survival probability of nonlinear oscillators endowed with fractional derivative element and subjected to evolutionary excitation: A stochastic averaging treatment with path integral concepts, Probab. Eng. Mech. 66 (2021) 103156.
[23] J. Roberts, J. Dunne, A. Debonos, Stochastic estimation methods for non-linear ship roll motion, Probab. Eng. Mech. 9 (1) (1994) 83–93.
[24] J. Roberts, M. Vasta, Markov modelling and stochastic identification for nonlinear ship rolling in random waves, Philos. Trans. R. Soc. A: Math. Phys. Eng. Sci. 358 (2000) 1917–1941.
[25] R.L. Bagley, P.J. Torvik, A theoretical basis for the application of fractional calculus to viscoelasticity, J. Rheol. 27 (3) (1983) 201–210.
[26] I. Podlubny, Fractional Differential Equations, Mathematics in Science and Engineering, Vol. 198, Academic Press, San Diego, ISBN: 978-0-12-558840-9, 1999.
[27] F. Mainardi, Fractional Calculus and Waves in Linear Viscoelasticity: An Introduction to Mathematical Models, Imperial College Press, London, ISBN: 978-1-84816-330-0, 2010.
[28] V.C. Fragkoulis, I.A. Kougioumtzoglou, A.A. Pantelous, M. Beer, Non-stationary response statistics of nonlinear oscillators with fractional derivative elements under evolutionary stochastic excitation, Nonlinear Dynam. 97 (4) (2019) 2291–2303.

[29] P. Ni, I.P. Mitseas, V.C. Fragkoulis, M. Beer, Spectral incremental dynamic methodology for nonlinear structural systems endowed with fractional derivative elements subjected to fully non-stationary stochastic excitation, Struct. Saf. 111 (2024) 102525.
[30] P.D. Spanos, B.A. Zeldin, Random vibration of systems with frequency-dependent parameters or fractional derivatives, J. Eng. Mech. 123 (3) (1997) 290–292.
[31] I.P. Mitseas, P. Ni, V.C. Fragkoulis, M. Beer, Survival probability surfaces of hysteretic fractional order structures exposed to non-stationary code-compliant stochastic seismic excitation, Eng. Struct. 318 (2024) 118755.
[32] C.T. Ngoc, S.-D. Lee, S.-S. You, X. Xu, Active control synthesis of nonlinear pitch–roll motions for marine vessels under regular waves, Ocean Eng. 221 (2021) 108537.
[33] A. Di Matteo, Response of nonlinear oscillators with fractional derivative elements under evolutionary stochastic excitations: A path integral approach based on Laplace's method of integration, Probab. Eng. Mech. 71 (2023) 103402.
[34] B. Pomaro, P.D. Spanos, Extended statistical linearization approach for estimating non-stationary response statistics of systems comprising fractional derivative elements, Probab. Eng. Mech. 74 (2023) 103471.
[35] Z. Xing, L. Mccue, Modeling ship equations of roll motion using neural networks, Nav. Eng. J. 122 (3) (2010) 49–60.
[36] International Code on Intact Stability, International Maritime Organization, London, UK, 2008.
[37] J.M. Falzarano, Z. Su, A. Jamnongpipatkul, A. Somayajula, Solving the problem of nonlinear ship roll motion using stochastic dynamics, in: V.L. Belenky, K.J. Spyrou, F. van Walree, M. Almeida Santos Neves, N. Umeda (Eds.), Contemporary Ideas on Ship Stability: Risk of Capsizing, Springer International Publishing, Cham, 2019.
[38] A.B. of Shipping, Guide for Fatigue Assessment of Offshore Structures, American Bureau of Shipping, Houston, TX, 2020.
[39] C. Jiang, A.W. Troesch, S.W. Shaw, Capsize criteria for ship models with memory-dependent hydrodynamics and random excitation, Philos. Trans. R. Soc. A: Math. Phys. Eng. Sci. 358 (2000) 1761–1791.
[40] K. Hasselmann, T. Barnett, E. Bouws, H. Carlson, D. Cartwright, K. Enke, J. Ewing, H. Gienapp, D. Hasselmann, P. Kruseman, A. Meerburg, P. Müller, D. Olbers, K. Richter, W. Sell, H. Walden, Measurements of Wind-Wave Growth and Swell Decay During the Joint North Sea Wave Project (JONSWAP), Tech. Rep. 12, 1973, Dtsch. Hydrogr. Z., Suppl.A8.
[41] E. Branlard, Generation of Time Series from a Spectrum: Generation of Wave Times Series from the JONSWAP Spectrum, Tech. Rep., Risø DTU, National Laboratory for Sustainable Energy, 2010.
[42] I. Senjanović, G. Ciprić, J. Parunov, Survival analysis of fishing vessels rolling in rough seas, Philos. Trans. R. Soc. A: Math. Phys. Eng. Sci. 358 (2000) 1943–1965.
[43] I.A. Kougioumtzoglou, Y. Zhang, M. Beer, Softening Duffing oscillator reliability assessment subject to evolutionary stochastic excitation, ASCE-ASME J. Risk Uncertain. Eng. Syst. A: Civ. Eng. 2 (2) (2015) 04015002.
[44] R. Rajaraman, G. Hariharan, Estimation of roll damping parameters using Hermite wavelets: An operational matrix of derivative approach, Ocean Eng. (ISSN: 0029-8018) 283 (2023) 115031.
[45] A. Rezaei, M. Tabatabaei, Ship roll stabilization using an adaptive fractional-order sliding mode controller, Ocean Eng. (ISSN: 0029-8018) 287 (2023) 115883.
[46] M. Taylan, The effect of nonlinear damping and restoring in ship rolling, Ocean Eng. 27 (9) (2000) 921–932.
[47] J. Wright, W. Marshfield, Ship roll response and capsize behaviour in beam seas, Trans. R. Inst. Nav. Archit. 122 (1979) 129–148.
[48] I.P. Mitseas, O. Danisworo, Stochastic seakeeping analysis of nonlinear ship rolling dynamics under non-stationary and irregular sea states, Comput. Struct. 323 (2026) 108164.
[49] I.A. Kougioumtzoglou, P.D. Spanos, An approximate approach for nonlinear system response determination under evolutionary stochastic excitation, Current Sci. 97 (2009) 1203–1211.
[50] I.P. Mitseas, M. Beer, First-excursion stochastic incremental dynamics methodology for hysteretic structural systems subject to seismic excitation, Comput. Struct. 242 (2021) 106359.
[51] W. Li, L. Chen, N. Trisovic, A. Cvetkovic, J. Zhao, First passage of stochastic fractional derivative systems with Power-Form restoring force, Int. J. Non-Linear Mech. 71 (2015) 83–88.
[52] P.D. Spanos, A. Di Matteo, Y. Cheng, A. Pirrotta, J. Li, Galerkin Scheme-Based determination of survival probability of oscillators with fractional derivative elements, J. Appl. Mech. 83 (12) (2016) 121003.
[53] I.P. Mitseas, Y. Zhang, V.C. Fragkoulis, Risk assessment of block random rocking on nonlinear foundation subject to evolutionary seismic ground motion, Mech. Syst. Signal Process. 240 (2025) 113397.
[54] J.B. Roberts, P.D. Spanos, Stochastic averaging: an approximate method of solving random vibration problems, Int. J. Non-Linear Mech. 21 (2) (1986) 111–134.
[55] P.D. Spanos, L.D. Lutes, Probability of response to evolutionary process, J. Eng. Mech. Div. 106 (2) (1980) 213–224.
[56] I.P. Mitseas, I.A. Kougioumtzoglou, P.D. Spanos, M. Beer, Nonlinear MDOF structural system survival probability determination subject to evolutionary stochastic excitation, Strojnisk Vestnik-J. Mech. Eng. 62 (7–8) (2016) 440–451.
[57] P.-T.D. Spanos, G.P. Solomos, Markov approximation to transient vibration, J. Eng. Mech. 109 (4) (1983) 1134–1150.
[58] J.L. Beck, C. Papadimitriou, Moving resonance in nonlinear response to fully nonstationary stochastic ground motion, Probab. Eng. Mech. 8 (3–4) (1993) 157–167.
[59] J.B. Roberts, P.D. Spanos, Random Vibration and Statistical Linearization, Courier Corporation, 2003.
[60] I.P. Mitseas, M. Beer, Modal decomposition method for response spectrum based analysis of nonlinear and non-classically damped systems, Mech. Syst. Signal Process. 131 (2019) 469–485.
[61] S. Sutulo, C. Guedes Soares, On applicability of mathematical models based on fractional calculus to ship dynamics, IFAC Proc. Vol. 43 (20) (2010) 190–195.
[62] S. Surendran, J.V.R. Reddy, Numerical simulation of ship stability for dynamic environment, Ocean Eng. 30 (10) (2003) 1305–1317.
[63] S. Kianejad, H. Enshaei, J. Duffy, N. Ansarifard, Prediction of a ship roll added mass moment of inertia using numerical simulation, Ocean Eng. 173 (2019) 77–89.
[64] M. Shinozuka, G. Deodatis, Simulation of stochastic processes by spectral representation, ASME Appl. Mech. Rev. 44 (4) (1995) 191–204.
[65] K. Oldham, J. Spanier, The Fractional Calculus Theory and Applications of Differentiation and Integration to Arbitrary Order, Elsevier, 1974.